

## Article

# Effect of Thermal Mismatch on Fracture Characteristics of Porcelain Veneered Lithia-Based Disilicate Posterior Ceramic Crown

Ja-Young Kim <sup>1,†</sup>, Yu-Kyoung Kim <sup>2,†</sup>, Won-Suk Oh <sup>3</sup>, Tae-Sung Bae <sup>2</sup>, Jung-Jin Lee <sup>1</sup>, Min-Ho Lee <sup>2</sup>, Yong-Seok Jang <sup>2,\*</sup> and Seung-Geun Ahn <sup>1,\*</sup> 

<sup>1</sup> Department of Prosthodontics, School of Dentistry, Jeonbuk National University, Jeonju 54896, Republic of Korea

<sup>2</sup> Department of Dental Biomaterials, Institute of Biodegradable Materials, School of Dentistry, Jeonbuk National University, Jeonju 54896, Republic of Korea

<sup>3</sup> Department of Biologic and Materials Sciences and Prosthodontics, University of Michigan School of Dentistry, Ann Arbor, MI 48109, USA

\* Correspondence: yjang@jbnu.ac.kr (Y.-S.J.); sgahn@chonbuk.ac.kr (S.-G.A.)

† Ja-Young Kim and Yu-Kyoung Kim contributed equally to this study and should be considered co-first authors.

**Abstract:** (1) Background: Dental glass–ceramics shrink during crystallization, complicating restoration manufacturing. Thermo-pressure molding was introduced to address this, with lithium disilicate crystals providing high strength. Residual tensile stresses can influence the chipping strength of single tooth crowns. (2) Methods: Insync dentine was layered onto three lithia-based disilicate core ceramics (Amber Press, IPS e.max Press) for microtensile bond strength tests. The Vickers test assessed the residual tensile stress and interfacial bonding. Porcelain-veneered posterior ceramic crowns were fabricated and subjected to axial loading, measuring fracture loads (three per group). (3) Results: A chemical bonding layer formed at the interface, which was thicker in the Insync-IPS e.max Press and increased with more firings. The ultimate tensile bond strength was 28.5 MPa for the four-times-fired Insync-Amber Press, similar to the twice-fired Insync-IPS e.max Press. No residual tensile stress was found in the Insync-Amber Press; the Insync-IPS e.max Press showed crack growth within 250 µm of the bonded interface. The average fracture resistance was twice as high for the Insync-Amber Press. (4) Conclusions: The Insync-Amber Press exhibited better thermal harmony with no crack growth, while the IPS e.max Press showed crack growth due to residual tensile stress. Insync-Amber Press posterior ceramic crowns had significantly greater fracture resistance than Insync-IPS e.max Press crowns.

**Keywords:** veneering porcelain; disilicate core ceramic; dental ceramic crown; fracture resistance



**Citation:** Kim, J.-Y.; Kim, Y.-K.; Oh, W.-S.; Bae, T.-S.; Lee, J.-J.; Lee, M.-H.; Jang, Y.-S.; Ahn, S.-G. Effect of Thermal Mismatch on Fracture Characteristics of Porcelain Veneered Lithia-Based Disilicate Posterior Ceramic Crown. *Appl. Sci.* **2024**, *14*, 9682. <https://doi.org/10.3390/app14219682>

Academic Editor: Maria Antoniadou

Received: 12 September 2024

Revised: 17 October 2024

Accepted: 18 October 2024

Published: 23 October 2024



**Copyright:** © 2024 by the authors. Licensee MDPI, Basel, Switzerland. This article is an open access article distributed under the terms and conditions of the Creative Commons Attribution (CC BY) license (<https://creativecommons.org/licenses/by/4.0/>).

## 1. Introduction

Glass–ceramic restorations are renowned for their translucency and esthetic appeal. However, castable glass–ceramics pose challenges in fabricating ceramic restorations due to contraction during the crystallization heat treatment process. Additionally, their strength and fracture toughness are not significantly different from conventional feldspathic porcelains [1]. Microcracks of the porcelain can expand due to stresses generated by thermal contraction, leading to a vicious cycle that further degrades the durability of the coated porcelain. When cracks occur, the resistance to occlusal forces decreases, causing additional damage. Therefore, understanding the interaction among these factors is crucial for enhancing the performance of all-ceramic crowns [2]. In recent years, heat-pressed methods have been introduced to address these shortcomings. This technique utilizes ingots that have undergone pre-crystallization heat treatment, offering advantages such as

precise manufacturing, low porosity, excellent marginal adaptation, and higher strength and Weibull coefficient compared to conventional sintering methods [3].

Glass-ceramic materials utilized in heat-pressed methods include leucite, apatite, and lithium disilicate crystals. Although materials containing precipitated leucite and apatite crystals provide excellent esthetics, they exhibit lower fracture strength, restricting their use primarily to inlays, onlays, and single crowns for anterior teeth [4]. In contrast, materials reinforced with lithium disilicate crystals boast strengths exceeding 400 MPa, making them suitable for single crown restorations in both anterior and posterior teeth. For anterior restorations prioritizing esthetics, a dual-layered all-ceramic crown with feldspathic porcelain over the core is commonly employed [5].

In addition, as for the latest dental ceramic trends, zirconia is a very strong ceramic with a strength of over 1000 MPa, and the latest transparent zirconia is used for both anterior and posterior crowns to improve both esthetics and durability [6]. Hybrid ceramics are a mixture of polymer and ceramic used to increase flexibility and shock absorption, making them advantageous for immediate application, and resin nano ceramics enhance strength and durability through ceramic nano particles to show wear characteristics similar to natural teeth [7]. In addition, multilayer ceramics are popular as products that enhance esthetic perfection with various layers [8].

Although the dual-layered all-ceramic crown is esthetically pleasing, it has been associated with issues such as chipping of the veneered porcelain and cracking or fractures within the core and at the bonding interface [9,10]. Glass-ceramic restorations have shown fracture patterns in both the veneered porcelain and the core [11]. These challenges can potentially be mitigated by increasing the thickness of the ceramic in areas prone to high tensile stress, optimizing the structural support between the veneered porcelain and the core, and minimizing porosity within the sintered body and micro-gaps at the bonding interface [12]. Microcracks on the surface or bonding interface are primary contributors to veneered porcelain chipping. Dental ceramic materials typically exhibit low elastic energy absorption capacities, making them prone to crack propagation even under low tensile stresses when microcracks are present. These microcracks often originate from defects such as the poor surface finishing of veneered porcelain or inadequate bonding with the core, ultimately compromising the restoration's durability. Moreover, inconsistent heat shrinkage between the veneered porcelain and the core can generate stress during mastication, further promoting crack propagation [12–14].

The aim of this study was to evaluate the fracture properties of posterior lithium disilicate ceramic crowns veneered with porcelain. Microtensile bond strength testing was conducted to measure bond strength and assess interfacial bonding quality affected by the thermal mismatch between the veneering porcelain and two core ceramics. The null hypothesis tested whether there was a significant difference in fracture resistance between the two groups of posterior lithium disilicate ceramic crowns under compressive axial loading.

## 2. Materials and Methods

Two lithia disilicate-based core ceramics, Amber Press MO1 ingot (Hass, Gangneung, Republic of Korea) and IPS e.max Press MO1 ingot (Ivoclar-Vivident, Schaan, Liechtenstein), were used to fabricate ceramic blocks as substrates for a feldspathic veneering porcelain, Insync dentine A2 (Jensen Industrial Inc., North Haven, CT, USA), in the present *in vitro* study.

### 2.1. Measurement of Microtensile Bond Strength of Veneering Porcelain to Lithia Disilicate Based Core Ceramic

Six acrylic resin blocks (Pattern Resin, GC Corporation, Tokyo, Japan) measuring  $10 \times 10 \times 5$  T (mm) were prepared using a mold and randomly divided into 2 groups (3 blocks per group). A sprue former was attached to each resin block and secured to the crucible former for investment. The investment material (Prime Vest HS, BK Giulini,

Ludwigshafen, Germany) was mixed with a water/powder ratio of 0.25 and allowed to set at room temperature for 30 min. The resin blocks were burned out at 850 °C for 50 min. Each group of ceramic core materials, Amber Press MO1 (FCF22 JF0901, Hass, Gangneung, Republic of Korea) and IPS e.max Press MO1 (T14564, Ivoclar/Vivadent, Schaan, Liechtenstein), was heat-pressed under ambient conditions and cooled to room temperature. The ceramic blocks were divested using airborne particle abrasion technology with 50 µm glass beads (Rolloblast, Renfert GmbH, Hilzingen, Germany) at 2 atmospheres and then polished with silicon carbide (SiC) abrasive papers ranging from 240 to 2000 grit. After polishing, the ceramic blocks were cleaned in an ultrasonic bath with distilled water for 5 min and dried in a 50 °C for 1 h.

The prepared lithia-based disilicate core ceramic blocks were layered with InSync Dentine A2 veneering porcelain. The polished surface of the core ceramic was thinly coated with the veneering porcelain. The porcelain was mixed with an exclusive solution and fired at 765 °C for 1 min for the primary firing. Additional layers of veneering porcelain were incrementally added in thickness, and the specimens underwent 2 more firing cycles to achieve final dimensions of 10 × 10 × 5 T (mm) (Table 1).

**Table 1.** Materials information and firing schedule for specimen preparation.

| Materials           | Company                         | Flexural Strength (MPa) | CTE ( $10^{-6}/^{\circ}\text{C}$ ) | ST (°C) | TRI (°C/min) | FT (°C) | HT (min) | V1 (°C) | V2 (°C) |
|---------------------|---------------------------------|-------------------------|------------------------------------|---------|--------------|---------|----------|---------|---------|
| Amber Press MO1     | Hass, Republic of Korea         | 460                     | 10.2                               | 700     | 60           | 920     | 15       | 700     | 920     |
| IPS e.Max Press MO1 | Ivoclar-Vivident, Liechtenstein | 400                     | 10.6                               | 700     | 60           | 915     | 15       | 500     | 915     |
| InSync Dentine A2   | Jensen Industrial Inc., USA     | 250                     | 8.7                                | 400     | 40           | 760     | 1 (air)  | 450     | 760     |

CTE: coefficient of thermal expansion; ST: starting temperature; FT: final temperature; TRI: temperature rate increase; V1: vacuum on; V2: vacuum off; HT: holding time.

The prepared ceramic specimens were mounted on a slow-speed diamond cutter (Metsaw-LS, Topmet, Daejeon, Republic of Korea) and serially sectioned perpendicular to the porcelain-to-core ceramic interface (1 × 1 × 10 mm). Four ceramic bar specimens were taken from the middle of each ceramic block and immersed in distilled water at 37 °C for 24 h for hydrothermal aging. The bar specimens were attached to metal holders using cyanoacrylate adhesive and subjected to tensile force at a crosshead speed of 0.5 mm/min in a universal testing machine (5569, Instron Co., Norwood, MA, USA). The load at the moment of fracture failure of each test specimen was measured to calculate the tensile bond strength (MPa), with the fracture load (N) divided by the cross-sectional area (mm<sup>2</sup>) of each specimen.

## 2.2. Residual Tensile Stress Resulting from Thermal Mismatch

Six acrylic resin blocks (Pattern resin, GC Corporation, Tokyo, Japan) (10 × 10 × 1 mm in dimension) were prepared using a mold and randomly divided into 2 groups. A sprue former was attached to each resin block and secured to the crucible former for investment. The investment and heat-press molding of ceramic core materials (Amber Press MO1 and IPS e.max Press MO1) were performed following the procedure. The finished core ceramic blocks were layered with a veneering porcelain (InSync dentine A2). The veneering porcelain was layered 3 times and fired as recommended by the manufacturer for preparation of a layered ceramic specimen. Each prepared specimen was embedded in an acrylic resin and secured to a slow-speed diamond cutter (Metsaw-LS) and sectioned transversely at a right angle to the interface of veneering porcelain to core ceramic. Each sectioned specimen was polished with SiC abrasive papers to 2000 grit. To remove any micro-defects formed during the polishing process, final polishing was performed with 1 µm diamond paste. The fracture toughness of the ceramics was evaluated

using the indentation method using the Vickers pyramid. The prepared ceramic specimen was secured to a microhardness tester (Micro Vickers hardness tester, Mityutoyo, Takatsu, Japan). The Vickers indenter was pressed into the core ceramic adjacent to the interface with veneering porcelain. The loading was delivered under a press-in load of 9.8 N and holding time of 15 s to measure the length of the initial crack. The ceramic indentation made by the Vickers indenter and the crack growth were analyzed by an optical microscope.

### 2.3. Fracture Resistance Test of Posterior Veneered Ceramic Crown

A digital scanner (D900L, 3Shape, Copenhagen, Denmark) was used to scan a model of the maxillary right first molar (Figure 1a). An abutment core for a posterior ceramic crown was custom designed and milled from metal (Ti or Co-Cr alloy) using a milling machine M1 (Zirkonzahn, South Tyrol, Italy). Milling wax (Wax ivory 95H10, Zirkonzahn, South Tyrol, Italy) was processed to prepare 20 copings, randomly assigned to two groups of core ceramics (10 samples each) (Figure 1b). The wax copings were fixed to the crucible former by attaching a sprue former, and each of the 10 Amber Press MO1 and IPS e.max Press MO1 ceramic copings were prepared by thermal pressing of the ceramic cores according to the procedure described in the previous section (Figure 1c). To produce a layered structure, the ceramic coping was thinly veneered with a feldspathic porcelain (Insync dentine A2). The primary firing of the porcelain was conducted at 765 °C for 1 min, and 2 additional layers were added with dentine A2 powder and enamel59 A3.5 powder to obtain a dimension, as depicted in Figure 2a. The veneered lithia-based disilicate ceramic crown was fired and glazed at 720 °C for 1 min, as shown in Figure 2b.

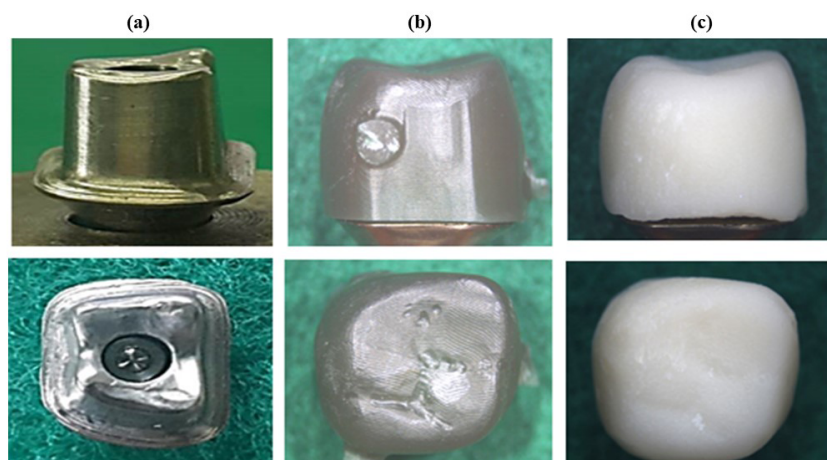


**Figure 1.** Preparation of ceramic core specimen for fracture resistance (lateral and above direction): (a) custom milled abutment, (b) milled wax coping, and (c) pressed ceramic coping.

The prepared ceramic crowns were bonded to the metal abutment. The abutment was treated with a 32% phosphoric acid gel (Scotchbond Universal Etchant, 3M/ESPE, Neuss, Germany), and the internal aspect of the ceramic crown was etched with 9.5% hydrofluoric acid gel (Porcelain Etchant 9.5% HF, BISCO, Schaumburg, IL, USA). The metal abutment was brushed with MDP primer (Z-PRIME PLUS, Bisco, Schaumburg, IL, USA), and the etched surface of ceramic crown was coated with silane primer (ESPE Sil, 3M/ESPE, Neuss, Germany) and dried lightly with a dryer for 3 s. The crowns were luted to the abutment with a double polymerization resin cement (Rely-X U200, 3M/ESPE, Neuss, Germany) under a static compressive loading of 49 n force in an upright position. The prepared posterior ceramic crown specimen was secured to a holding device and loaded axially to fail by fracture in a universal testing machine (4201, Instron, Canton, MA, USA). A steel ball with a diameter of 3 mm was placed in the central fossa of the crown and lined up with the center of the load bar. A compressive force was applied at a crosshead speed of

0.5 mm/min, and the load at the moment of fracture of the crown was recorded, as shown in Figure 2c.

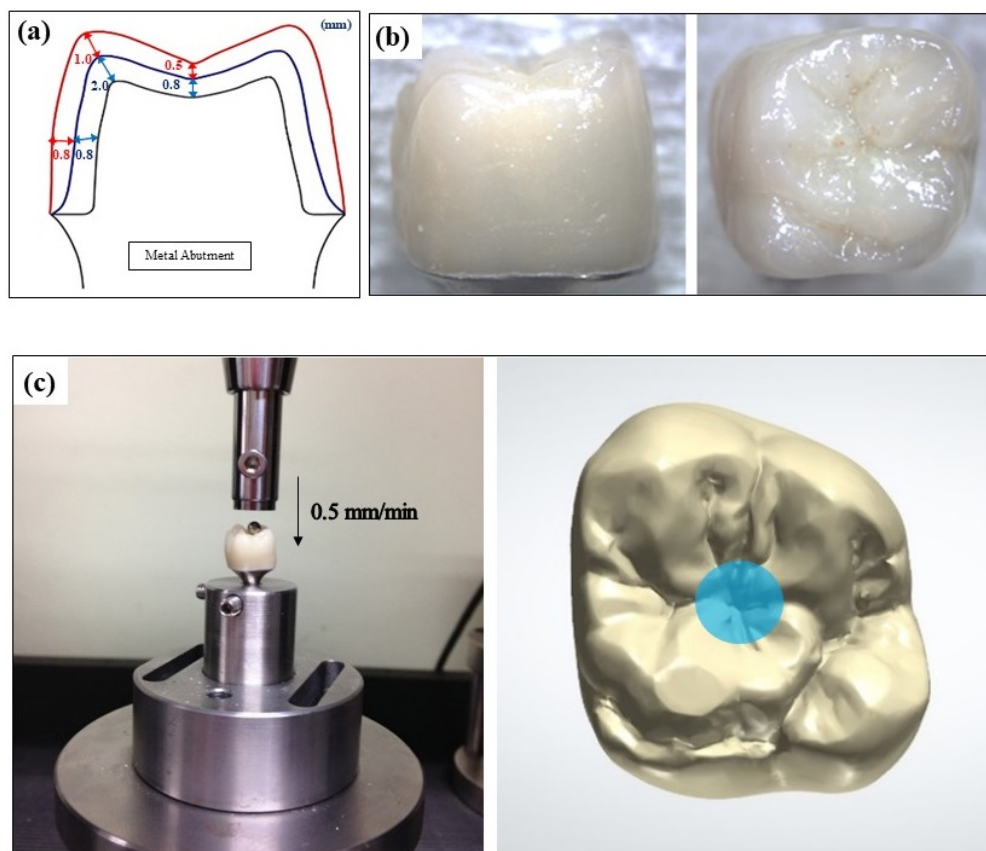


**Figure 2.** Schematic diagram: (a) a dimension of a posterior veneered ceramic crown, (b) veneered lithium-based disilicate ceramic crown (lateral and above direction), and (c) compressive loading applied to ceramic crown.

#### 2.4. Imaging Analysis

A pattern of crack growth associated with the indents made in the core ceramic adjacent to the interface was analyzed to evaluate the residual stress resulting from a thermal mismatch between the veneering porcelain and core ceramic. The morphological microstructure was analyzed using high-resolution field emission scanning electron microscopy (HR FE-SEM, SU8230, Hitachi, Chiyoda, Japan).

#### 2.5. Statistical Analysis

The data were analyzed for statistical significance ( $p < 0.05$ ) using a one-way analysis of variance (ANOVA) and *t*-test.

### 3. Results

The lithium-based disilicate core ceramic observed after firing three layers of veneer porcelain (Insync dentine A2) has a needle-shaped crystal structure, as shown in Figure 3. Amber Press MO1 has a denser and finer crystal pattern than IPS e.max Press MO1. Figure 3a–f display a picture observed with the Insync-Amber Press and Insync-IPS e.max Press groups, focusing on the reaction layer at the bonding interface, and Figure 3g is the result showing the number of firings and the thickness of the reaction layer. The thickness of the reaction layer increased linearly as the number of firing times increased, and a large number of pores were observed. As for the thickness of the reaction layer, the Insync-IPS e.max Press group tended to be thicker than the Insync-Amber Press group.

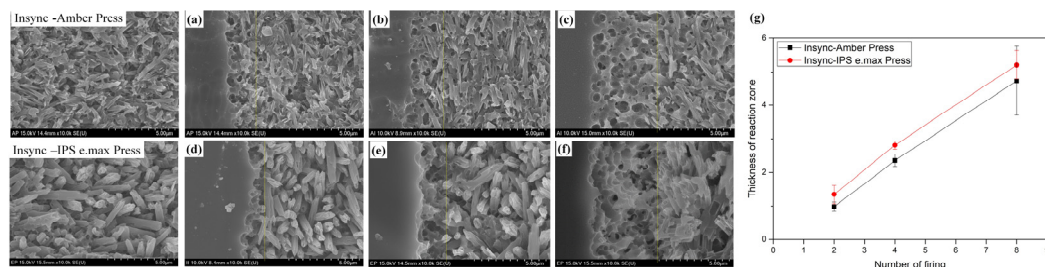


**Figure 3.** The morphologies of crystal structure of lithia-based disilicate core ceramics after firing of a veneer porcelain (Insync dentine A2) and reaction zone of veneered porcelain to lithia-based disilicate core ceramic. (a–c) Insync-Amber Press interfaces; (d–f) Insync-IPS e.max Press interfaces. Firing (a,d) 2 times, (b,e) 4 times, and (c,f) 8 times and (g) number of firings and thickness of reaction layer at bonding interface.

Figure 4 shows the microtensile bond strength of Insync-Amber Press and Insync-IPS e.max Press specimens according to the number of firings. As the number of firings of veneered porcelain increased to two, four, and eight times, the Insync-Amber Press group showed the highest bonding strength of  $28.5 \pm 8.6$  MPa in the fourth firing group. On the other hand, in the Insync-IPS e.max Press group, the highest value was  $28.3 \pm 9.4$  MPa in the second firing group, and a statistically significant difference was shown in the second and eighth firing groups ( $p < 0.05$ ). The eighth firing group of Insync-IPS e.max Press all fractured during production.

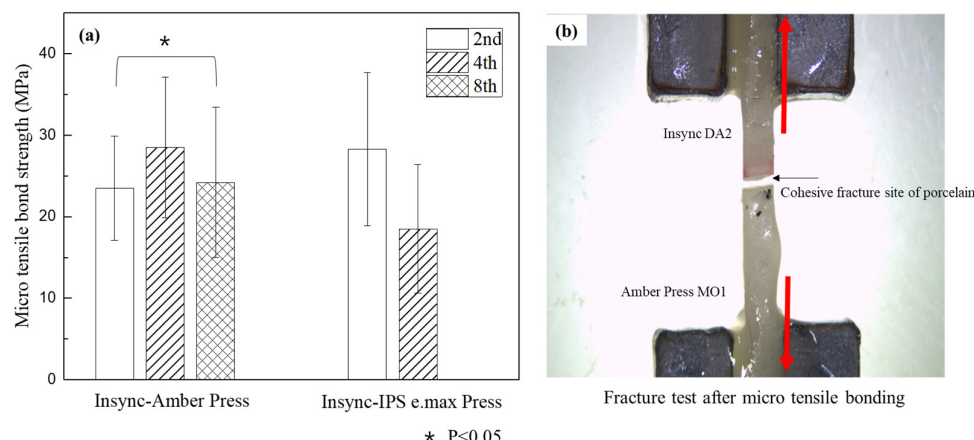
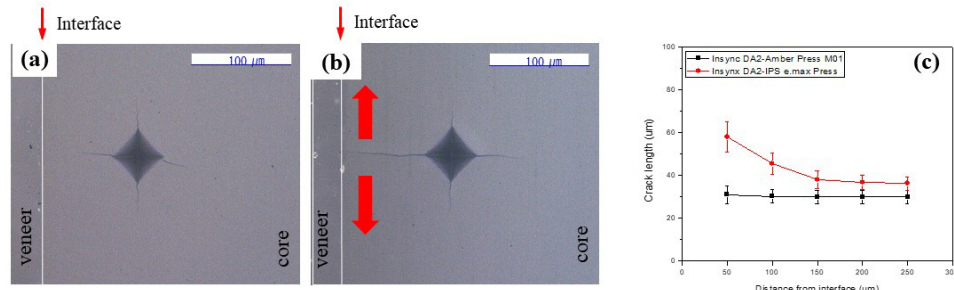


**Figure 4.** (a) Means and standard deviations of the microtensile bond strength values, and (b) the model of fracture test after micro tensile bonding.

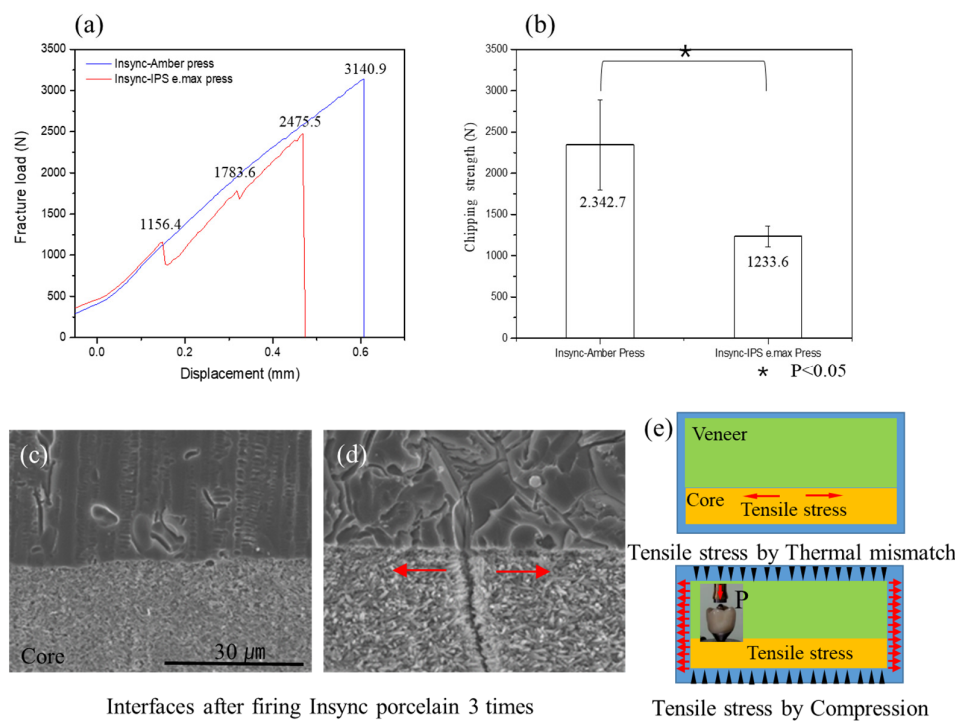
Figure 5 shows the relationship between the indentation location and the crack length according to the distance from the bonding interface in each group. In the Insync-Amber Press specimen, the initial crack length did not change with the distance from the interface. However, in the Insync-IPS e.max Press specimen, the crack length decreased as the distance from the interface increased, and the effect was found over a range of about 250  $\mu\text{m}$  from the bonding interface.

Figure 6a shows the load–displacement curve when an external force is applied by placing a steel ball with a diameter of 3 mm in the center of the occlusal surface of the Insync-Amber Press and Insync-IPS e.max Press crown specimens. In the Insync-Amber Press crown, chipping did not occur, and the crown was fractured, but in the Insync-IPS e.max Press crown, chipping occurred several times from a relatively low load stage, and then the crown fractured. Figure 6b shows the initial chipping strength of the Insync-Amber Press crown and Insync-IPS e.max Press crown specimens, which were  $2342.7 \pm 543.2$  N and  $1233.6 \pm 125.5$  N, respectively, and there was a statistically significant difference between them ( $p < 0.05$ ). Additionally, as a result of measuring the chipping strength of the two

experimental groups, the null hypothesis of the study was rejected. This is because the chipping strength of the Insync-IPS e.max Press crown, where residual tensile stress was observed in the lithium disilicate core, is lower than that of the Insync-Amber Press crown.



**Figure 5.** Initial crack growth with the Vickers indenter pressed into the core ceramic adjacent to the bonded interface: (a) Insync-Amber Press, (b) Insync-IPS e.max Press, and (c) relationship between distance from interface and initial crack length during indentation with Vickers indenter.



**Figure 6.** (a) Load–displacement curve, (b) chipping strength value, sectional views of bonded interface after 3 firings of veneering porcelain (Insync) as (c) Insync-Amber Press, (d) Insync-IPS e.max Press (the red arrows: direction of stress), and (e) direction of tensile stress due to applied external force types.

Figure 6c,d show the indentations and initial cracks created after indenting a Vickers indenter with a load of 9.8 N and a holding time of 15 s into the core 100 μm away from the bonding interface of the Insync-Amber Press and Insync-IPS e.max Press specimens. In the case of Amber Press, the crack length formed along the edge of the indentation was symmetric in all directions, and from this, it can be assumed that residual tensile stress did not occur. However, in the case of IPS e.max Press, cracks in the direction perpendicular to the bonding interface were generated longer than in other directions, indicating that residual tensile stress occurred due to thermal mismatch between the Insync ceramic material and IPS e.max Press. Figure 6c,d show the observation of the bonding interface after firing Insync three times. In the Insync-Amber Press, cracks are not visible on the

inner surface of the core, but in the Insync-IPS e.max Press specimen, cracks due to tensile stress can be seen in the core.

#### 4. Discussion

In this study, lithia-based heat-pressed ceramic copings of Amber Press MO1 and IPS e.max Press MO1 were layered with Inync veneering porcelain to produce a double layered structure. The double layers were found to establish a chemical bonding, as indicated by a reaction layer at the interface of the bonding. The reaction layer area of the Insync-IPS e.max Press group showed a thicker difference than that of the Insync-Amber Press group. Studies have shown that the thicker reactive layer of thermo-pressed ceramic coping results in lower heat diffusivity and lower resistance to fracture [15]. In addition, a thick reaction layer is prone to microcracks or defects and, especially under load, becomes brittle due to stress concentrations, which increases the risk of fracture [16].

A thermal mismatch may play a critical role in retaining the stability of the interfacial bonding of a veneering porcelain to core ceramic. The veneering porcelain exists as viscoelastic at a high temperature during firing and becomes solid during cooling below the glass transition temperature. Because of the phase transformation, residual stress may develop in a veneered ceramic restoration [17]. Also, the cooling of veneer ceramic restorations may not occur uniformly, as the outer surface of the ceramic exposed to the surrounding air may cool faster than the inner surface, but residual stresses may occur throughout the veneer structure of the ceramic restoration [18].

That is, a mismatch in the coefficient of the thermal expansion of a veneering porcelain may develop residual tensile stress in the core ceramic adjacent to the interface of bonding and cause a chipping or fracture under occlusal loading [19]. A sintered veneering porcelain may also demonstrate inherent defects or pores of stress concentrators at the subsurface or at the interface of bonding. According to a previous study, a slight compressive stress built in the layered structure can be conducive to suppressing the development of a crack, leading to chipping or fracture [20]. However, the criteria for an appropriate range of thermal mismatch of a veneering porcelain to core ceramic are unclear. Clinical prediction studies using the Viscoelastic Finite Element Method (VFEM) to address this issue have shown that thick ceramic layers can lead to strong stress gradients, which can easily propagate cracks due to contact damage. Therefore, the interaction between the thickness ratio and residual stress is more relevant to the susceptibility to chipping than bulk fracture [21].

The thermal expansion coefficient of Insync dentine veneering porcelain was  $8.7 \times 10^{-6}/^{\circ}\text{C}$ , and that of Amber Press and IPS e.max Press core ceramics was  $10.2 \times 10^{-6}/^{\circ}\text{C}$  and  $10.6 \times 10^{-6}/^{\circ}\text{C}$ , respectively. Thus, the thermal mismatch was  $1.5 \times 10^{-6}/^{\circ}\text{C}$  in the Insync-Amber Press group and  $1.9 \times 10^{-6}/^{\circ}\text{C}$  in the Insync-IPS e.max Press group. In the present study, the veneering porcelain was fired three times to investigate the pattern of crack propagation under the Vickers indenter pressed within the range of approximately 250  $\mu\text{m}$  from the bonded interface.

The Vickers indentation method involved in this study is widely used to characterize the residual stress of brittle materials such as small and irregularly shaped dental ceramic restorations [22,23]. In the present study, the ceramic specimen was finely polished to demonstrate a flat surface to meet the requirement of the testing method. For the Insync-Amber Press group, the pattern of a crack that formed along the edges of the indentation was symmetrical in all directions, indicating no accumulation of a residual tensile stress resulting from the thermal mismatch. However, an accumulation of a residual tensile stress was evident in the Insync-IPS e.max Press group, where the crack that developed toward the interface of bonding was longer than the other sides of the indentation. These findings may indicate a negative impact on the core ceramic driven by greater than a certain limit of residual stress resulting from the thermal mismatch of veneering porcelain to core ceramic [24]. In addition, the core ceramic specimen was found to demonstrate numerous microcracks after being subjected to porcelain firing four times.

Porcelain fracture can occur in the area of functional cusps or marginal ridges that may lack a support by the core substrate [12]. In addition, the micro-gaps existing in the interface of the bonding of a veneering porcelain to core ceramic may play a role as concentrators of high tensile stress. A fracture may develop at the point of the most vulnerable defect. However, the defects are scarce at the interface of chemical bonding established through the chemical interaction of veneered porcelain to core ceramic. According to a previous study, the level of stress was reduced by enhancing the characteristics of fracture resistance when the interfacial bonding was established through chemical interactions of a veneering porcelain to core ceramic [25].

In the present study, the veneered porcelain was fired multiple times to a lithia-based disilicate core ceramic to investigate the impact of porcelain firing on the characteristics of the interfacial bonding. Interestingly, the bond strengths of each group of the investigation were inconsistent by varying the number of firing cycles. The bonding of the Insync-Amber Press group was most stable ( $28.5 \pm 8.6$  MPa) when it underwent four firing cycles, whereas the Insync-IPS e.max Press group showed the greatest bond strength ( $28.3 \pm 9.4$  MPa) when the veneered porcelain was fired twice. In general, multiple firing rounds may adversely affect the fracture characteristics of veneered ceramic restoration [26]. The reaction layer was thicker when the number of firing cycles was increased. There were a greater number of pores in the thicker reaction layer, compromising the interfacial bonding and reducing the fracture resistance of a veneered posterior ceramic crown.

Axial loading was applied by means of a steel ball placed in the central fossa of the posterior ceramic crown specimen. The fracture load and the initial chipping strength of the Insync-Amber Press was higher than the Insync-IPS e.max Press group. This suggests a significant difference in the failure resistance between the two groups. Also, the reaction layer of the Insync-IPS e.max Press group was thicker, which resulted in increased residual tensile stresses and consequently lower fracture resistance. Within the limitations of the testing environment, no veneer chipping was observed in the Insync-Amber Press crown group. In contrast, the Insync-IPS e.max Press crown group exhibited a pronounced pattern of veneer chipping, even under relatively low levels of loading. In other words, the reaction layer in the Insync-IPS e.max Press group was thicker, which resulted in a higher residual tensile stress, and this stress concentration leads to brittleness and an increased risk of fracture under load [15]. Various characteristics of ceramic failure are related to residual tensile stresses accumulated in the core ceramic adjacent to the bonded interface, and it was confirmed that thermal expansion mismatch and bonding properties affect the performance of the ceramic restoration [27].

The actual force that human teeth can withstand varies depending on the location of the teeth. On average, the occlusal force (the force that teeth receive when chewing) of adults is about 200 to 500 N, and it can reach up to 800 N, especially in the molar area where food is ground [28]. It is said that maxillary premolars can fracture under a load of 1121 N, and sound molars can fracture under a load of about 2500 N [29]. In this study, the fracture strength of the lithia-based disilicate core ceramic material was more than 3140 N (Insync-Amber Press), which is sufficient to withstand the force applied to molars.

This study was conducted under in vitro conditions, which did not take into account various factors that may occur in the actual oral environment. The load in the oral cavity, including moisture and temperature fluctuations, is constantly changing. In addition, the thickness of the reaction layer and the number of craters were not maintained the same in each group, which may lead to errors in the interpretation. These methodological limitations may have a significant impact on the interpretation of the study results and their clinical applicability. Therefore, future studies should supplement these factors to obtain more reliable results.

Understanding the influence of the thickness and thermal properties of the reaction layer on the long-term stability of the ceramic can help predict the lifetime of the ceramic material in clinical practice. In addition, understanding the influence of the thickness of

the reaction layer on the durability and fracture resistance of the ceramic can improve the design and manufacturing methods of dental ceramics used in clinical practice.

## 5. Conclusions

This study investigated the fracture resistance and bonding properties of posterior lithium disilicate ceramic crowns veneered with Insync porcelain.

1. The Insync-IPS e.max Press group had a significantly thicker reaction layer than the Insync-Amber Press group. This was linked to lower thermal diffusivity, increased brittleness, and stress concentration, resulting in residual tensile stresses and higher fracture risk.
2. Chemical interaction was observed at the bonding interface, with the Insync-IPS e.max Press group showing cracks within 250  $\mu\text{m}$  of the interface, while the Insync-Amber Press group exhibited no residual tensile stresses.
3. The failure load of Insync-Amber Press crowns was significantly higher than that of Insync-IPS e.max Press crowns, underscoring the importance of matching thermal expansion and achieving strong chemical bonding for improved durability.

In conclusion, reaction layer thickness and thermal properties are crucial in determining the fracture resistance of all-ceramic crowns.

**Author Contributions:** Conceptualization, J.-Y.K.; methodology, Y.-K.K., W.-S.O. and T.-S.B.; performing animal experiments, T.-S.B., J.-Y.K. and Y.-K.K.; writing—original draft preparation, J.-J.L. and T.-S.B.; writing—review and editing, Y.-K.K. and M.-H.L.; project administration, Y.-S.J. and S.-G.A. All authors have read and agreed to the published version of the manuscript.

**Funding:** This research received no external funding.

**Institutional Review Board Statement:** Not applicable.

**Informed Consent Statement:** Not applicable.

**Data Availability Statement:** Data may be available upon reasonable request to the corresponding author.

**Acknowledgments:** HR FE-SEM were obtained at the JeonJu Center of KBSI, and this study has reconstructed the data of Ji-Hoon Lee's doctoral dissertation. This study was supported by the research grant from Hass, Gangneung, Gangwon-do, Republic of Korea.

**Conflicts of Interest:** The authors declare no conflicts of interest.

## References

1. Giordano, R.; McLaren, E.A. Ceramics overview: Classification by microstructure and processing methods. *Compend. Contin. Educ. Dent.* **2010**, *31*, 682. [[PubMed](#)]
2. Rekow, E.D.; Silva, N.R.F.A.; Coelho, P.G.; Zhang, Y.; Guess, P.; Thompson, V.P. Performance of Dental Ceramics: Challenges for Improvements. *J. Dent. Res.* **2011**, *90*, 937–952. [[CrossRef](#)]
3. Zhang, Y.; Lawn, B.R. Novel Zirconia Materials in Dentistry. *J. Dent. Res.* **2018**, *97*, 140–147. [[CrossRef](#)]
4. Holand, W.; Schweiger, M.; Frank, M.; Rheinberger, V. A comparison of the microstructure and properties of the IPS Empress®2 and the IPS Empress® glass-ceramics. *J. Biomed. Mater. Res.* **2000**, *53*, 297–303. [[CrossRef](#)]
5. Guess, P.C.; Zavanelli, R.A.; Silva, N.R.F.A.; Bonfante, E.; Coelho, P.G.; Thompson, V.P. Monolithic CAD/CAM lithium disilicate versus veneered Y-TZP crowns: Comparison of failure modes and reliability after fatigue. *Int. J. Prosthodont.* **2010**, *23*, 434–442. [[PubMed](#)]
6. Alqutaibi, A.Y.; Ghulam, O.; Krsoum, M.; Binmahmoud, S.; Taher, H.; Elmalky, W.; Zafar, M.S. Revolution of Current Dental Zirconia: A Comprehensive Review. *Molecules* **2022**, *27*, 1699. [[CrossRef](#)] [[PubMed](#)]
7. Dadkhah, M.; Tulliani, J.-M.; Saboori, A.; Iuliano, L. Additive manufacturing of ceramics: Advances, challenges, and outlook. *J. Eur. Ceram. Soc.* **2023**, *43*, 6635–6664. [[CrossRef](#)]
8. Contreras, L.P.C.; Rodrigues, C.S.; Zucuni, C.P.; Valandro, L.F.; Marocho, S.M.S.; de Melo, R.M. Fatigue behavior of multilayer ceramic structures in traditional and reverse layering designs. *J. Prosthodont.* **2024**, *33*, 389–395. [[CrossRef](#)] [[PubMed](#)]
9. Sailer, I.; Pjetursson, B.E.; Zwahlen, M.; Hämmmerle, C.H.F. A systematic review of the survival and complication rates of all-ceramic and metal-ceramic reconstructions after an observation period of at least 3 years: Part II: Fixed dental prostheses. *Clin. Oral Implant. Res.* **2007**, *18*, 86–96. [[CrossRef](#)]

10. Al-Dohan, H.M.; Yaman, P.; Dennison, J.B.; Razzoog, M.E.; Lang, B.R. Shear strength of core-veneer interface in bi-layered ceramics. *J. Prosthet. Dent.* **2004**, *91*, 349–355. [[CrossRef](#)]
11. Marquardt, P.; Strub, J.R. Survival rates of IPS Empress 2 all-ceramic crowns and fixed partial dentures: Results of a 5-year prospective clinical study. *Quintessence Int.* **2006**, *37*, 253–259. [[PubMed](#)]
12. Zhao, K.; Pan, Y.; Guess, P.C.; Zhang, X.P.; Swain, M.V. Influence of veneer application on fracture behavior of lithium-disilicate-based ceramic crowns. *Dent. Mater.* **2012**, *28*, 653–660. [[CrossRef](#)] [[PubMed](#)]
13. Isgrò, G.; Pallav, P.; van der Zel, J.M.; Feilzer, A.J. The influence of the veneering porcelain and different surface treatments on the biaxial flexural strength of a heat-pressed ceramic. *J. Prosthet. Dent.* **2003**, *90*, 465–473. [[CrossRef](#)] [[PubMed](#)]
14. AlShehri, S.A.; Mohammed, H.; Wilson, C.A. Influence of lamination on the flexural strength of a dental castable glass ceramic. *J. Prosthet. Dent.* **1996**, *76*, 23–28. [[CrossRef](#)]
15. Zarone, F.; Di Mauro, M.I.; Ausiello, P.; Ruggiero, G.; Sorrentino, R. Current status on lithium disilicate and zirconia: A narrative review. *BMC Oral Health* **2019**, *19*, 134. [[CrossRef](#)]
16. Vasiliu, R.-D.; Porojan, S.D.; Porojan, L. In Vitro Study of Comparative Evaluation of Marginal and Internal Fit between Heat-Pressed and CAD-CAM Monolithic Glass-Ceramic Restorations after Thermal Aging. *Materials* **2020**, *13*, 4239. [[CrossRef](#)]
17. Tholey, M.J.; Swain, M.V.; Thiel, N. Thermal gradients and residual stresses in veneered Y-TZP frameworks. *Dent. Mater.* **2011**, *27*, 1102–1110. [[CrossRef](#)] [[PubMed](#)]
18. Swain, M.V. Unstable cracking (chipping) of veneering porcelain on all-ceramic dental crowns and fixed partial dentures. *Acta Biomater.* **2009**, *5*, 1668–1677. [[CrossRef](#)]
19. De Carvalho, M.A.; Boaventura, M.; Costa, T.; Neris, N.; Rocha, A.A.; Lazari, P.C. Influence of the coefficient of thermal expansion on the stress distribution in ceramic veneers after thermal simulation. *Int. J. Adv. Eng. Res. Sci.* **2020**, *7*, 429–435. [[CrossRef](#)]
20. Coffey, J.P.; Anusavice, K.J.; Dehoff, P.H.; Lee, R.B.; Hojjatie, B. Influence of Contraction Mismatch and Cooling Rate on Flexural Failure of Pfm Systems. *J. Dent. Res.* **1988**, *67*, 61–65. [[CrossRef](#)]
21. Rodrigues, C.S.; Dhital, S.; Kim, J.; May, L.G.; Wolff, M.S.; Zhang, Y. Residual stresses explaining clinical fractures of bilayer zirconia and lithium disilicate crowns: A VFEM study. *Dent. Mater.* **2021**, *37*, 1655–1666. [[CrossRef](#)] [[PubMed](#)]
22. Marshall, D.B.; Lawn, B.R. An Indentation Technique for Measuring Stresses in Tempered Glass Surfaces. *J. Am. Ceram. Soc.* **1977**, *60*, 86–87. [[CrossRef](#)]
23. Park, J.-M.; Bae, T.-S.; Song, K.-Y.; Park, C.-W. An evaluation of the crack propagation characteristics of porcelain and the bond stress of ceramo-metal system. *J. Korean Acad. Prosthodont.* **1994**, *32*, 47–76.
24. Pereira, R.M.; Ribas, R.G.; Montanheiro, T.L.D.A.; Schatkoski, V.M.; Rodrigues, K.F.; Kito, L.T.; Kobo, L.K.; Campos, T.M.B.; Bonfante, E.A.; Gierthmuehlen, P.C.; et al. An engineering perspective of ceramics applied in dental reconstructions. *J. Appl. Oral Sci.* **2023**, *31*, e20220421. [[CrossRef](#)]
25. Daou, E.E. The zirconia ceramic: Strengths and weaknesses. *Open Dent. J.* **2014**, *8*, 33–42. [[CrossRef](#)]
26. Cetik, S.; Vincent, M.; Atash, R. Effect of Cosmetic Ceramics on Fracture Toughness of All-Ceramic Restorations. *J. Dent.* **2018**, *15*, 137–142.
27. Lohbauer, U.; Scherrer, S.S.; Della Bona, A.; Tholey, M.; van Noort, R.; Vichi, A.; Kelly, J.R.; Cesar, P.F. ADM guidance-Ceramics: All-ceramic multilayer interfaces in dentistry. *Dent. Mater.* **2017**, *33*, 585–598. [[CrossRef](#)]
28. Shala, K.; Tmava-Dragusha, A.; Dula, L.; Pustina-Krasniqi, T.; Bicaj, T.; Ahmed, E.; Lila, Z. Evaluation of Maximum Bite Force in Patients with Complete Dentures. *Open Access Maced. J. Med. Sci.* **2018**, *6*, 559–563. [[CrossRef](#)]
29. Göktürk, H.; Karaarslan, E.S.; Tekin, E.; Hologlu, B.; Sarikaya, I. The effect of the different restorations on fracture resistance of root-filled premolars. *BMC Oral Health* **2018**, *18*, 196. [[CrossRef](#)]

**Disclaimer/Publisher's Note:** The statements, opinions and data contained in all publications are solely those of the individual author(s) and contributor(s) and not of MDPI and/or the editor(s). MDPI and/or the editor(s) disclaim responsibility for any injury to people or property resulting from any ideas, methods, instructions or products referred to in the content.